Benha Journal of Applied Sciences (BJAS) **print: ISSN 2356–9751**
Vol. (9) Issue (9) (2024), (33- 42) **online: ISSN 2356–976x**
http://bjas.bu.edu.eg

Impact of Susceptibility Weighted MRI Sequences in Cerebral Small Vessel Disease

Alaa A. Hamad, Hisham A. Al-Sheikh and Mohamed A. Tawfik
Department of Radiodiagnosis, Faculty of Medicine, Benha University
E-mail: hmdla8801@gmail.com

Abstract

Background: Brain microvascular disease (CSVD) is a multifactorial condition affecting the brain's arterioles, venules, capillaries, and microscopic arteries. Susceptibility-weighted imaging (SWI) is a fully velocity-compensated high-resolution 3D gradient-echo sequence that creates new contrast sources using magnitude and filtered-phase data. This study aimed to weighed MRI sequences for CSVD susceptibility evaluation. Methods: SVD patients with CSVD were studied in this prospective observational study. Every patient had a comprehensive clinical evaluation, routine laboratory testing, susceptibility weighted MRI (SWI), and determination of the plasma atherogenic index. Results: The stroke-to-MRI time was longer in patients with one or more vascular clusters (P=0.028). Radiological investigation revealed no significant difference in WMH scores, however patients with vascular clusters had bigger lacunes, PVH + DWMH Fazekas score, basal ganglia + centrum semiovale PVS score, and overall PVS score (P<0.05). In multivariate logistic regression, the only significant predictors of vessel-clusters were age, male sex, and lacune amount. Conclusion: It seems that vascular clusters might be useful in risk stratification and individualised treatment for lacunar stroke. To find out how vessel-clusters impact clinical outcomes over time, further research is required.

Keywords: Cerebral Small Vessel Disease, Sequences, Weighted MRI, Susceptibility.

Introduction

Numerous disorders may cause cerebral small vascular disease (CSVD), which is characterised by damage to the brain's tiny arteries, arterioles, venules, and capillaries. In essence, CSVD is homogenous; it causes age-related disability, cognitive decline, and stroke. Numerous investigations have been conducted on CSVD. (1). CSVD neuroimaging may reveal recent tiny subcortical infarcts, lacunes, hyperintensities of white matter, perivascular spaces, microbleeds, and brain atrophy (2). The primary symptoms of chronic spondyloema virus (CSVD) are irregular gait, cognitive decline, dementia, mental problems, and stroke (3).

By using filtered-phase and magnitude data, susceptibility-weighted imaging (SWI) creates new sources of contrast. This 3D gradient-echo sequence has great resolution and is fully velocity-corrected. In less than four minutes, SWI is able to scan the whole brain using clinical 3T MR images and parallel imaging. (4).

The use of SWI in addition to conventional MR imaging sequences can improve evaluation of neurologic disorders such as traumatic brain injury (TBI), coagulopathic or other hemorrhagic disorders, cerebral infarction, neoplasms, and neurodegenerative disorders associated with intracranial calcification or iron deposition. (5).

It may be possible to find neuroimaging indicators for SVD by using SWI MRI. It is possible to accurately detect neurodegeneration by looking for iron-containing compounds in brain tissue analysis. (6).

Using SWI intensity units—0 denoting Galen's veins and 200 CSF—the hypointensity of the targeted area is assessed during image processing (7).

Iron is necessary for neurometabolism in the brain in the form of neuromelanin, but too much of it may be hazardous. Age-related changes in neural tissue iron transport may result in an iron buildup. Excessive iron intake results in lipid peroxidation, free radicals, and nerve injury. (8).

This research examined the impact of susceptibility weighted MRI sequences on CSVD.

Patients and methods

From May to December 2023, CSVD patients with SVD were the subjects of this prospective observational study conducted at the neurological department of Benha University Hospitals.

Written informed consent was provided by patients. Each patient received a code number and an explanation of the study's objective. The investigation was approved by the research ethics committee of Benha University Faculty of Medicine.

Inclusion criteria were age 65–90 years old, both sexes, presence of leukareosis of any severity and/or one or more lacunar infarctions in neuroimaging, acute or subacute signs of SVD [the primary criteria were neuroimaging features of SVD because clinical symptoms of SVD are more heterogeneous and typically mild at the onset of cerebral SVD (7)], and acute ischaemic stroke subtype SVDs and large vessel disease (LVDs) were diagnosed on cranial CT and M.

Exclusion criteria were clinical dementia, clinical parkinsonism, intracranial haemorrhage, intracranial

space-occupying lesion, psychiatric disease interfering with cognitive testing, acetylcholine-esterase inhibitors, neuroleptic agents, L-dopa, or dopa-a(nta)gonists, non-SVD-related wmls, severe visual and hearing impairment, MRI contraindications, and gait and balance disorders unrelated to

Every patient under study underwent the following: gathering demographic information, such as height, weight, body mass index (BMI), sex, and age. Full clinical history, including [smoking and the presence of medical morbidities such as diabetes mellitus, dyslipidaemia, hypertension, chronic kidney disease, coagulopathy, deep vein thrombosis or varicose veins, history of prior transient ischaemic attack episodes, and maintenance on any medications]. BMI was calculated and patients were classified into overweight patients ≥ 25 and obese patients ≥ 30 (grade I (30–34.99), grade II (35–34.99), and grade III ≥ 40). Full clinical presentation with [dizziness, headache, tired muscles, weak handgrip, numb feet, forgetfulness, and lethargy] and impaired vision and speech. Full clinical examination including measurements of heart rate, temperature, pulse, and systolic and diastolic blood pressure. Frequent laboratory tests include lipid profiles (total cholesterol, triglycerides, high density lipoproteins (HDL-s) and low density lipoproteins (LDL-s), coagulation profile testing, thyroid function testing, and complete blood counts. Radiological investigations: [MRI (SWI) weighted for susceptibility).

A lipid indicator called the plasma atherogenic index was used to assess each patient. The base-10 logarithm of the TG to HDL-C concentration ratio in milligrammes per litre is known as the AIP. TC less HDL-C is non-HDL-C. The ratio of non-HDL-C to HDL-C is known as the atherogenic index (AI). The ratio of TC×TG×LDL to HDL-C is known as the lipoprotein combine index (9). AC: (total cholesterol−HDLc)/HDLc, CRI-I: total cholesterol/HDLc, CRI-II: LDLc/HDLc, Total cholesterol − HDL is non-HDLc. In 24-hour spot urine samples, formulas were used to estimate the mean urinary excretion of Na and K.

Using an ultrafast 3D SWI sequence with the following parameters: TE/TR = 21.5/40 ms, voxel size = 0.9x0.9x1.8 mm3, Wave-CAIPI acceleration R = 6, scan time = 100 s (10), all patients underwent brain imaging on a Siemens Healthcare 3 Tesla Skyra MRI scanner. We obtained traditional T1, T2, FLAIR, and DWI. Two board-certified neuroradiologists, J.C. and S.Y.H., looked over the SWI data separately. A microbleed anatomical evaluation scale that is simplified was used to quantify the sites of abnormal susceptibility signals (11). After counting to ten, raters record lesions that are "greater than ten" per anatomical location.

SWI sequencing protocol with MRI:

Axial TSE T1-axial-weighted image (TR 400 ms TE 14 ms flip angle, 90°), axial and coronal TSE T2-weighted image (WI, TR 2500 ms TE 88 ms flip angle, 90°), axial and sagittal FLAIR FS (TR 9000 ms TE 127 Diffusion-sensitizing gradients), axial SWI (TR 78 ms TE 47 ms flip angle 15°slice thickness 1.5 mm), magnitude and phase images, and post-processing were among the sequences utilised to create SWI and MIP (12).

Qualitative examination of images:

Using the STRIVE criteria2, lacunes, PVS, microbleeds, and WMH were found on structural MRI sequences. These results were assessed in the basal ganglia and centrum semiovale using the PVS load scale and the Fazekas scale, a recognised qualitative measure for WMH. The pre-study photos were centralised and examined by an analyst who was blind to patient data and CVR findings, and who was not involved in clinical evaluations. How the vessel-like structures connected spatially to the anterior and posterior horns of the lateral ventricles (anterior, middle, and posterior white matter) and if they formed a linear rim around the margins of a cavitation in the white matter. After brain areas of interest were segmented, each vessel cluster's volume (mL) and form (round, ovoid, linear, or irregular) were measured. The vessel-cluster brain regions were classified according to previous research14: fully cavitated lesions with liquid that resembles cerebrospinal fluid (CSF), partially cavitated WMH (with a lacy appearance or incomplete cavities connected by residual tissue strands), and normal-appearing white matter. On structural sequences, clusters and related tissue form.

Image quantitative analysis:

The standardised white matter haemoglobin (WMH) volume was calculated using our intracranial, seemingly normal-appearing WMH volumes. For the purpose of analysing CVR magnitude and latency in both normal-looking white matter and WMH, we decreased the outer border of the original white matter mask by 2.5 mm (1 voxel) in order to minimise partial volume effects. We used a dilated ventricle mask to exclude images of normal arteries running along the ventricle walls and ventricular cerebrospinal fluid (CSF). Lastly, we used the initial vessel-cluster segmentations to create three more 3D expansions (shells) surrounding the vessel-clusters. Each shell is 2 voxels thick in T2-w space, which is equivalent to 1 voxel in CVR data. We restricted these expansions to the white matter in order to evaluate the magnitude and delay of CVR in

the surrounding tissue. After that, we used an algorithm to generate white matter segments that were mirror-images of each other, checked their location, and made any necessary human adjustments (E.C. and S.R.). The FLS16 was used for mask processing.

Statistical analysis:

It was SPSS v28 (IBM©, Armonk, NY, USA) that was used to do the statistical analysis. Checking for data normality was done using Shapiro-Wilks and histograms. The mean and standard deviation were used as parametric quantitative data, and the unpaired student t-test was used for analysis. The median and interquartile range (IQR) were used for non-parametric quantitative data analysis in the Mann Whitney U test. Qualitative variables, such as frequency and percentage (%), were analysed using the Chi-square test or Fisher's exact test, if appropriate. The presence of significance was shown by a two-tailed P value less than 0.05. Finding out how many independent variables were associated with a dependent variable was the goal of multivariate logistic regression.

Cases

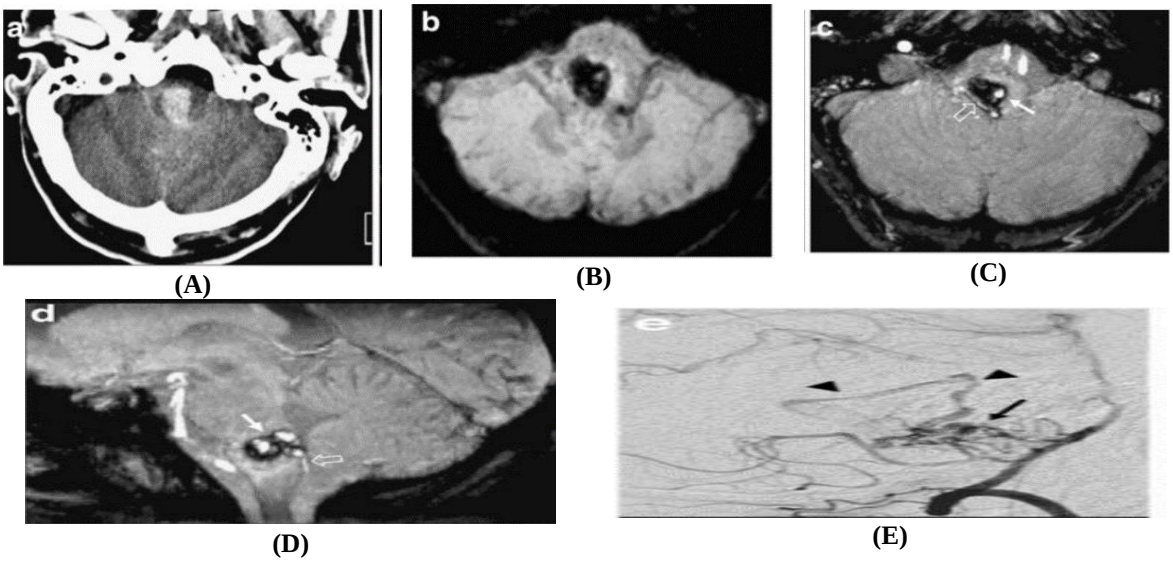

Fig (1: a) CT shows an acute hemorrhagic lesion located in the medulla oblongata. b The SWI minIP image clearly depicts the brainstem hemorrhage, which is markedly hypointense. c, d SWI, axial and reformatted sagittal images, processed with a maximum intensity projection algorithm (MIP), show flow-related enhancement within the hemorrhagic lesion (arrow) and a hypertrophied right posterior inferior cerebellar artery (PICA; open arrow) which are consistent with a small ruptured brainstem AVM. e Cerebral angiography, selective injection of the right vertebral artery: brainstem AVM (arrow) fed by branches of the right PICA and early venous drainage into a cerebellar vein (arrowheads)

Figure 1 The 43-year-old patient's brainstem haemorrhage is shown by CT, which indicates an acute medulla oblongata lesion. The SWI minIP picture shows hypointense brainstem haemorrhage. SWI, axial, and reconstructed sagittal images produced with a maximum intensity projection technique demonstrate flow-related increase in the haemorrhagic lesion and a hypertrophied right posterior inferior cerebellar artery, indicating a tiny, ruptured brainstem AVM. Right vertebral artery injection is selectively shown by cerebroangiography.

Results

Table (1) Baseline characteristics, medical history, clinical examination of vital signs, laboratory examinations and lipid profile of the studied patients

		Total (n=40)
Age (years)	**Mean± SD**	77.7 ± 6.59
	Range	65 - 89
Sex	**Male**	25 (62.5%)
	Female	15 (37.5%)
Weight (Kg)	**Mean± SD**	72.7 ± 10.73
	Range	56 - 90
Height (m)	**Mean± SD**	1.6 ± 0.05
	Range	1.55 - 1.7
BMI (Kg/m^2)	**Mean± SD**	27.7 ± 4.6
	Range	21.34 - 36.63
Medical history	**Hypertension**	23 (57.5%)
	Diabetes mellitus	11 (27.5%)
	Hyperlipidemia	19 (47.5%)
	Smoking	19 (47.5%)
	Ischemic heart disease	7 (17.5%)
	Peripheral vascular disease	3 (7.5%)
	Statin use	16 (40%)
	Antiplatelet use	23 (57.5%)
HR (beats/min)	**Mean± SD**	84.8 ± 9.45
	Range	71 - 100
SBP (mmHg)	**Mean± SD**	137.5 ± 14.1
	Range	120 - 160
DBP (mmHg)	**Mean± SD**	82.5 ± 8.4
	Range	70 - 90
Hb (g/dL)	**Mean± SD**	12.4 ± 0.54
	Range	11.5 - 13.5
Platelet ($*10^9/L$)	**Mean± SD**	280.4 ± 43.45
	Range	206 - 350
WBCs ($*10^9/L$)	**Mean± SD**	9.3 ± 1.5
	Range	6.5 - 11.5
Serum creatinine (mg/dL)	**Mean± SD**	0.5 ± 0.21
	Range	0.23 - 0.86
Urea (mg/dL)	**Mean± SD**	44.1 ± 10.5
	Range	25 - 60
ALT (U/L)	**Mean± SD**	36.9 ± 9.36
	Range	21 - 55
AST (U/L)	**Mean± SD**	33.9 ± 7.01
	Range	20 - 45
Total cholesterol (mg/dL)	**Mean± SD**	170.6 ± 40.05
	Range	100 - 238
Triglycerides (mg/dL)	**Mean± SD**	135.4 ± 26.63
	Range	91 - 177
HDL (mg/dL)	**Mean± SD**	47.3 ± 6.63
	Range	35 - 60
LDL (mg/dL)	**Mean± SD**	136.1 ± 21.64
	Range	95 - 168

BMI: body mass index. HR: heart rate, SBP: systolic blood pressure, DBP: diastolic blood pressure. Hb: haemoglobin,
WBCs: white blood cells, ALT: alanine aminotransferase, AST: aspartate aminotransferase. HDL: high density lipoprotein, LDL: low density lipoprotein.

Table 1 shows the baseline characteristics, medical history, clinical examination of vital signs, laboratory examinations and lipid profile of the studied patients

Table (2) Time from stroke to MRI, radiological data, and clusters analysis of the studied patients.

		Total (n=40)
Time from stroke to MRI (days)	**Mean± SD**	323.9 ± 139.33
	Range	88 - 542
Lacunes	**Mean± SD**	4.6 ± 2.84
	Range	0 - 9
	Median (IQR)	4.5 (2.75 – 7)
PVH + DWMH Fazekas score	**Mean± SD**	4.6 ± 1.15
	Range	3 - 6
	Median (IQR)	5 (3 - 5.25)
Basal ganglia PVS	**Mean± SD**	1.7 ± 0.54
	Range	1 - 2.5
	Median (IQR)	1.75 (1.375 – 2)
Basal ganglia + centrum semiovale PVS score	**Mean± SD**	4.5 ± 1.11
	Range	3 - 6
	Median (IQR)	4 (4 - 5.25)
Total PVS score	**Mean± SD**	2.5 ± 0.64
	Range	1.5 - 3.5
	Median (IQR)	2.5 (2 – 3)
Cerebral microbleeds	**Mean± SD**	3.9 ± 2.04
	Range	0 - 7
	Median (IQR)	3.75 (2.37 - 5.5)
Intracranial volume (mL)	**Mean± SD**	1.7 ± 0.54
	Range	1 - 2.5
	Median (IQR)	1.75 (1.37 – 2)
WMH (mL)	**Mean± SD**	11.2 ± 4.27
	Range	4.3 - 17.9
	Median (IQR)	10.25 (7.77 - 15.45)
CVR magnitude in normal appearing white matter CVR (%/mm Hg)	**Mean± SD**	0.04 ± 0.02
	Range	0 - 0.07
	Median (IQR)	0.031 (0.021 - 0.051)
CVR magnitude in WMH (%/mm Hg)	**Mean± SD**	0.1 ± 0.03
	Range	0.01 - 0.12
	Median (IQR)	0.063 (0.043 - 0.085)
CVR delay in normal appearing white matter (seconds)	**Mean± SD**	43.8 ± 14.73
	Range	19 - 69
CVR delay in WMH (seconds)	**Mean± SD**	36.5 ± 14.32
	Range	15 - 61
Clusters	**Yes**	15 (37.5%)
	No	25 (62.5%)
	Vessel-clusters (n=44)	
Location of vessel-clusters	**Left hemisphere**	17 (38.6%)
	Anterior deep white matter	8 (18.18%)
	Middle deep white matter	12 (27.27%)
	Posterior deep white matter	7 (15.90%)
Volume of the region containing the vessel-cluster (mL)	**Mean± SD**	0.18 ± 0.06
	Range	0.07 - 0.26
	Median (IQR)	0.18 (0.14 - 0.23)
Shape of vessel-clusters	**Round shape**	21 (47.72%)
	Ovoid	14 (31.81%)
	Irregular	3 (6.8%)
	Linear	7 (15.90%)

MRI: magnetic resonance imaging. CVR: cerebrovascular reactivity, DWMH: deep white matter hyperintensities, PVS: enlarged perivascular spaces, PVH: periventricular hyperintensities.

Table 2 Patient radiological data is shown. Time from stroke to MRI varied from 88 to 542 days, with a mean of 323.9 ± 139.33 days. In 15 individuals, 44 vessel-clusters were found, with 17 (38.6%) in the left hemisphere, 8 (18.18%) in the anterior, 12 (27.27%) in the centre, and 7 (15.90%) in the posterior deep white matter. The median (IQR) volume of the vessel-cluster area was 0.18 mL (0.14 - 0.23) and was round in 21 (47.72%), ovoid in 14 (31.81%), irregular in 3 (6.8%), and linear in 7 (15.90%). In the 44 vessel-clusters, 11 (29%) had clustered or linked low signal dots or lines that appeared to correspond to 1 main vessel-like structure, while 33 (75%), with a median of 2 (1–3) vessel-like structures per vessel cluster WNL/C29, had clusters of multiple structures. 7 (15.90%) were non-cavitated WMH, 20 (45.45%) were partial, and 17 (38.63%) were complete. Multi-vessel clusters, with a greater volume (median [IQR] volume [mL]: 0.58 [0.4–0.99] versus 0.31 [0.5–0.20], respectively, P <0.001), were linked to totally cavitated lesions.

Age and gender differences were minor. Patients with 1 or more vessel-clusters had a longer stroke-to-MRI time (P=0.028). Patients with 1 or more vessel-clusters had increased SBP and DBP (P=0.042, 0.037). Laboratory diagnosis was insignificant, but total cholesterol, triglycerides, and LDL were significantly elevated in patients with 1 or more vessel-clusters compared to those without (P=0.014, 0.018, 0.009), and HDL was significantly decreased (P=0.024). Radiological analysis showed greater lacunes, PVH + DWMH Fazekas score, basal ganglia + centrum semiovale PVS score, and total PVS score in patients with vessel-clusters (P<0.05), but no significant difference in WMH scores.

Table (3) Baseline characteristics, time from stroke to MRI, vital signs, laboratory diagnosis, lipid profile, and radiological data of the studied groups regarding the vessel-clusters

		Patients without vessel-clusters (n=25)	Patients with 1 or more vessel-clusters (n=15)	P value
Age (years)	**Mean± SD**	76.4 ± 6.81	79.7 ± 5.88	0.136
	Range	65 - 87	68 - 89	
Sex	**Male**	13 (52%)	8 (53.33%)	0.934
	Female	12 (48%)	7 (46.67%)	
Time from stroke to MRI (days)	**Mean± SD**	292.2 ± 147.81	392.8 ± 108.8	**0.028***
	Range	88 - 542	228 - 520	
SBP (mmHg)	**Mean± SD**	134.8 ± 13.27	144 ± 13.52	**0.042***
	Range	120 - 160	120 - 160	
DBP (mmHg)	**Mean± SD**	78.8 ± 8.81	84.7 ± 7.43	**0.037***
	Range	70 - 90	70 - 90	
Hb (g/dL)	**Mean± SD**	12.5 ± 0.56	12.4 ± 0.52	0.693
	Range	11.6 - 13.4	11.5 - 13.5	
Platelet (*10^9/L)	**Mean± SD**	283.1 ± 44.76	275.7 ± 42.29	0.609
	Range	206 - 349	210 - 350	
WBCs (*10^9/L)	**Mean± SD**	9.6 ± 1.47	8.7 ± 1.4	0.063
	Range	6.9 - 11.5	6.5 - 11.4	
Serum creatinine (mg/dL)	**Mean± SD**	0.53 ± 0.20	0.54 ± 0.22	0.921
	Range	0.23 - 0.86	0.26 - 0.84	
Urea (mg/dL)	**Mean± SD**	44.04 ± 10.66	44.07 ± 10.61	0.994
	Range	27 - 60	25 - 60	
ALT (U/L)	**Mean± SD**	36.5 ± 8.16	37.5 ± 11.37	0.761
	Range	22 - 52	21 - 55	
AST (U/L)	**Mean± SD**	34.4 ± 6.73	33.0 ± 7.61	0.548
	Range	22 - 45	20 - 44	
Total cholesterol (mg/dL)	**Mean± SD**	157.04 ± 37.85	189.6 ± 39.86	**0.014***
	Range	100 - 229	112 - 238	
Triglycerides (mg/dL)	**Mean± SD**	127.8 ± 26.21	148 ± 23.03	**0.018***
	Range	91 - 171	100 - 177	

HDL (mg/dL)	**Mean± SD**	49.4 ± 7.25	43.9 ± 7.1	**0.024***
	Range	35 - 60	35 - 57	
LDL (mg/dL)	**Mean± SD**	129.8 ± 21.14	147.7 ± 17.43	**0.009***
	Range	95 - 166	104 - 168	
Lacunes	**Mean± SD**	3.5 ± 2.5	6.5 ± 2.36	**<0.001***
	Range	0 - 9	2 - 9	
	Median (IQR)	3 (1 – 5)	7 (6 – 8)	
PVH + DWMH Fazekas score	**Mean± SD**	4.3 ± 1.21	5.1 ± 0.88	**0.035***
	Range	3 - 6	3 - 6	
	Median (IQR)	4 (3 – 5)	5 (5 - 6)	
Basal ganglia + centrum semiovale PVS score	**Mean± SD**	4.4 ± 1.04	5.1 ± 1.06	**0.050***
	Range	3 - 6	3 - 6	
	Median (IQR)	4 (4 – 5)	6 (4 – 6)	
Total PVS score	**Mean± SD**	2.3 ± 0.56	2.8 ± 0.7	**0.016***
	Range	1.5 - 3.5	1.5 - 3.5	
	Median (IQR)	2 (2 - 2.5)	3 (2 - 3.5)	
WMH (mL)	**Mean± SD**	11.2 ± 4.14	11.01 ± 4.61	0.867
	Range	4.7 - 17.9	4.3 - 17.7	
	Median (IQR)	10.3 (8.1 - 15.4)	9.6 (7.6 - 15.75)	

MRI: magnetic resonance imaging, *: statistically significant as P value <0.05. SBP: systolic blood pressure, DBP: diastolic blood pressure, *: statistically significant as P value <0.05. Hb: hemoglobin, WBCs: white blood cells, ALT: alanine aminotransferase, AST: aspartate aminotransferase. HDL: high density lipoprotein, LDL: low density lipoprotein, *: statistically significant as P value <0.05. DWMH: deep white matter hyperintensities, PVS: perivascular spaces, *: statistically significant as P value <0.05.

In Table 3, multivariate logistic regression analysis found that only age, male sex, and lacune number were significant predictors of vessel-cluster existence.

Table (4) Multivariate logistic regression analysis for prediction of the presence of vessel-clusters.

	OR	**95%CI**	**P value**
Age	1.1138	1.0101 to 1.2282	**0.031***
Sex	0.1667	0.0310 to 0.8968	**0.037***
BMI (Kg/m^2)	0.9783	0.8389 to 1.1408	0.779
Hypertension	10.9040	0.859 to 138.262	0.065
Diabetes mellitus	0.1900	0.0199 to 1.8114	0.149
Hyperlipidemia	1.0836	0.9661 to 1.2154	0.170
Smoking	1.0460	0.8715 to 1.2553	0.629
Ischemic heart disease	0.2017	0.0210 to 1.9395	0.165
Peripheral vascular disease	1.2471	0.0799 to 19.458	0.874
Statin use	0.3909	0.0318 to 4.8027	0.463
Antiplatelet use	0.9819	0.8895 to 1.0838	0.716
HR (beats/min)	1.0216	0.9530 to 1.0951	0.547
SBP (mmHg)	0.9843	0.9377 to 1.0332	0.521
DBP (mmHg)	1.0259	0.9457 to 1.1130	0.537
Hb (g/dL)	0.8629	0.2494 to 2.9857	0.815
Platelet ($*10^9/L$)	1.0083	0.9927 to 1.0243	0.298
WBCs ($*10^9/L$)	0.9748	0.6147 to 1.5458	0.913
Serum creatinine (mg/dL)	0.0865	0.0020 to 3.7275	0.202
Urea (mg/dL)	1.0118	0.9426 to 1.0862	0.745
ALT (U/L)	0.9957	0.9185 to 1.0794	0.917
AST (U/L)	1.0822	0.9613 to 1.2183	0.191
Total cholesterol (mg/dL)	0.9916	0.9746 to 1.0089	0.339
Triglycerides (mg/dL)	0.9803	0.9551 to 1.0062	0.134
HDL (mg/dL)	0.9861	0.8906 to 1.0918	0.787
LDL (mg/dL)	0.9917	0.9602 to 1.0242	0.611

Time from stroke to MRI (days)	1.0028	0.9976 to 1.0080	0.296
Lacunes	1.9959	1.3372 to 2.9791	**0.001***
PVH + DWMH Fazekas score	1.3105	0.6907 to 2.4865	0.235
Basal ganglia PVS	0.4001	0.1063 to 1.5053	0.175
Basal ganglia + centrum semiovale PVS score	0.7893	0.4168 to 1.4948	0.582
Total PVS score	0.8928	0.2927 to 2.7233	0.842
Cerebral microbleeds	0.7561	0.4834 to 1.1827	0.220
Intracranial volume (mL)	0.4841	0.1177 to 1.9919	0.314
WMH (mL)	1.0525	0.8729 to 1.2691	0.592
CVR magnitude in normal appearing white matter CVR (%/mm Hg)	1.0293	0.9571 to 1.1068	0.419
CVR magnitude in WMH (%/mm Hg)	0.9887	0.9432 to 1.0365	0.723
CVR delay in normal appearing white matter (seconds)	0.9505	0.8925 to 1.0122	0.113
CVR delay in WMH (seconds)	0.9935	0.9406 to 1.0494	0.815

OR: odds ratio, CI: confidence interval, BMI: body mass index, HR: heart rate, SBP: systolic blood pressure, DBP: diastolic blood pressure, Hb: hemoglobin, WBCs: white blood cells, ALT: alanine aminotransferase, AST: aspartate aminotransferase, HDL: high density lipoprotein, LDL: low density lipoprotein, DWMH: deep white matter hyperintensities, PVS: perivascular spaces, CVR: cerebrovascular reactivity, DWMH: deep white matter hyperintensities, PVS: enlarged perivascular spaces, PVH: periventricular hyperintensities, *: statistically significant as P value <0.05

Table 4

Discussion

The MRIs of the patients had a mean of 323.9 ± 139.33 days, with a range of 88 to 542 days, according to the research.

On the other hand, Pantoni (15) mostly found CMBs in the lobar brain areas.

In this research, lacunes varied from 0 to 9, with an average of 4.6 ± 2.84. The PVH + DWMH Fazekas score varied from 3 to 6 with a mean of 4.6 ± 1.15. Within a range of 1 to 2.5, the average basal ganglia PVS was 1.7 ± 0.54. The basal ganglia + centrum semiovale PVS score varied from 3 to 6, with a mean of 4.5 ± 1.11. The PVS score ranged from 1.5 to 3.5, with an average of 2.5 ± 0.64. The cerebral microbleeds had an average of 3.9 ± 2.04 and ranged from 0 to 7. The intracranial capacity had a mean of 1.7 ± 0.54 mL and varied from 1 to 2.5 mL. WMH readings varied from 4.3 to 17.9 mL, with a mean of 11.2 ± 4.27 mL. The typical seeming white matter CVR varied from 0 to 0.07 %/mm Hg, with a mean of 0.04 ± 0.02 %/mm Hg. The CVR magnitude in WMH varied from 0.01 to 0.12%/mm Hg, with a mean of 0.1 ± 0.03 %. The average CVR delay in normal white matter was 43.8 ± 14.73 seconds, with a range of 19 to 69 seconds. In WMH, the average CVR latency was 36.5 ± 14.32 seconds, with a range of 15 to 61 seconds.

According to Rudilosso et al. (14) (0–6.5), lacunes averaged three. PVH + DWMH= Fazekas mean 2 (1-3). Basal ganglia have an average PVS of 5 (3–6). For the centrum and basal ganglia, the semiovale PVS mean is 5 (3–6). Average PVS score: 2 (1-3). a microbleed of 0 to 3.5 in the brain. In-cranial capacity, the mean was 1412 (134) millilitres. The average WMH was 13.9 (5.6–53.7) mL. The mean CVR in seemingly normal white matter is 0.0351 (0.0359)%/mm Hg. WMH has an average CVR of 0.0569 (0.0692) %/mm Hg. 38.9 (23.8) seconds is the average white matter CVR latency, which is typical. The CVR delay at WMH is 44.54 (29.61) seconds on average.

During the current investigation of 15 individuals, 44 vessel-clusters were discovered. They were distributed as follows: 7 (15.90%) in the posterior deep white matter, 8 (18.18%) in the front, 12 (27.27%) in the middle, and 17 (38.6%) in the left hemisphere. The vessel-cluster area was ovoid in 14 (31.81%), irregular in 3 (6.8%), round in 21 (47.72%), and linear in 7 (15.90%), with a median volume of 0.18 mL (0.14 - 0.23).

Rudilosso et al. (2014) reported that 36 out of 76 patients (47%) had at least one vascular cluster, and 22 had several clusters with a fairly symmetrical distribution. 94 vessel-clusters were found in 36 individuals. There were 48 (51%) vessel-clusters in the left hemisphere, 22 (23%) in the anterior, 17 (18%) in the posterior deep white matter, and 55 (58.5%) in the middle. The median (IQR) volume of the vessel-cluster region was 0.15 mL (0.08–0.26). Of them, 45(48%) had round shapes, 32(34%) had irregular shapes, 11(12%) had oval shapes. With a median score of two out of three, the remaining 67 (71%), showed clusters of multiple vessel-like structures. 27 of the 94 vessel-clusters contained low signal dots or lines that seemed to be grouped together or joined to form a single, large vessel-like

structure (29%). Thirteen vessel-clusters (13%) were non-cavitated, forty-six (40%) were complete, and forty-five (48%) were incomplete. The position of white matter does not alter, even if vessel clusters—which have a linear rim appearance and are often linked to fully cavitated lesions—cover a greater volume than single-vessel-like structures. Each of the 12 vessel-clusters from non-cavitated areas had one main dilated vessel within WMH; nevertheless, the cavity margins of the partial and complete cavitated vessel clusters had a linear low-signal rim on SWI.

33 (75%) of the 44 vessel-clusters in this study showed clusters of multiple vessels, with a median of 2 (1-3) vessel-like structures per vessel cluster WNL/C29. In contrast, 11 (29%) of the 44 vessel-clusters showed clustered or connected low signal dots or lines that appeared to correlate to a single major vessel-like structure. Seven (15.90%) were non-cavitated WMH, twenty (45.45%) were partial, and seventeen (38.63%) were complete. Multi-vessel clusters with a higher volume (median [IQR] volume [mL]: 0.58 [0.4–0.99] versus 0.31 [0.5–0.20], respectively, P <0.001) were linked to fully cavitated lesions.

Vascular clusters on SWI may thus indicate that the small deep arteries are exhausted and unable to vasodilate, exacerbating tissue damage in those with sporadic or genetic SVD. Small parenchymal vessels look dark according to SWI vessel-cluster identification because of the paramagnetic distortion of the magnetic field brought on by deoxygenated haemoglobin (16).

The age and gender distributions within the study's groups varied substantially. Patients with one or more vascular clusters had a longer stroke-to-MRI time (P=0.028). Patients with one or more vascular clusters had increased SBP and DBP (P=0.042, 0.037).

CMBs were found in thirteen cortical, thirty-five deep, thirty-six mixed, and eighteen infra-tentorial individuals (Abou Elmaaty and Zarad, 2017). A statistically significant change was seen in SVDs ($\chi 2$ = 31.201, P < 0.001), and the frequency of CMBs in this experiment was 30% (68.8% in SVDs and 15.9% in LVDs).

The groups in this research had similar laboratory diagnoses (Hb, platelets, WBCs, serum creatinine, urea, ALT, and AST). substantially lower HDL (P=0.024) and substantially higher total cholesterol, triglycerides, and LDL (P=0.014, 0.018, 0.009) were seen in individuals with one or more vascular clusters compared to those without.

This is congruent with the observation by Mitaki and colleagues (18) that greater BMI was associated with higher deep and infra-tentorial CMBs, but still up for debate. Hypertension did not, however, cause an increase in CMBs.

In this research, the scores of patients with vascular clusters were considerably higher (p<0.001) on Lacunes, PVH + DWMH Fazekas, basal ganglia + centrum semiovale PVS, WMH, and total PVS. Rudilosso et al. found a significant (p<0.001) increase in the DWM Fazekas score, PVH + DWMH Fazekas score, basal ganglia PVS, centrum semiovale PVS, cerebral microbleeds, intracranial volume, WMH, Normalised WMH volume, CVR magnitude in normal appearing white matter, and CVR magnitude in WMH in patients with vessel-clusters.

The study's multivariate logistic regression analysis showed that age, male sex, and lacunes were the only factors that could predict vessel-clusters. Rudilosso et al. (14) found that vessel-clusters were not associated with age, sex, other vascular risk factors, or contemporaneous antithrombotic treatment, but rather with CADASIL, alcohol consumption, and worse SVD severity on structural imaging in the univariable analysis. Alcohol consumption and the CADASIL subtype stopped being able to predict vessel clusters in the multivariable analysis, and the only meaningful findings in structural imaging were lacunes and the normalised log10 WMH volume value. In the ordinal regression study, after correcting for confounders, the number of vascular clusters per patient remained substantially connected with male sex, lacunes, and the normalised log10 WMH volume value. On the other hand, both normal looking white matter and WMH had a nonsignificant downward trend in their CVR (percentage/100 mm Hg).

Conclusion

Lacunar stroke patients have shown the presence of vascular clusters as a neuroimaging signal. Significant white matter pathology, elevated blood pressure, and dyslipidaemia all pointed to a substantial cerebrovascular disease. Specifically, vessel-clusters were independently predicted by age, male sex, and lacune load. These findings suggest that vascular clusters may be useful in risk stratification and customised lacunar stroke treatment. To find out how vessel-clusters impact clinical outcomes over time, further research is required.

References

[1] Meng L, Zhao J, Liu J, Li S. Cerebral small vessel disease and cognitive impairment. Journal of Neurorestoratology. 2019;7:184-95.

[2] Zhao L, Lee A, Fan YH, Mok VCT, Shi L. Magnetic resonance imaging manifestations of cerebral small vessel disease: automated

quantification and clinical application. Chin Med J (Engl). 2020;134:151-60.
[3] Li Q, Yang Y, Reis C, Tao T, Li W, Li X, et al. Cerebral Small Vessel Disease. Cell Transplant. 2018;27:1711-22.
[4] Mittal S, Wu Z, Neelavalli J, Haacke EM. Susceptibility-weighted imaging: technical aspects and clinical applications, part 2. AJNR Am J Neuroradiol. 2009;30:232-52.
[5] Sahin N, Solak A, Genç B, Bilgiç N. Susceptibility-Weighted MR Imaging: Added value of susceptibility signals in diagnosis of hemorrhagic lesions of the brain. Turkish Journal of Cerebrovascular Diseases. 2014;20:77-86.
[6] Acosta-Cabronero J, Betts MJ, Cardenas-Blanco A, Yang S, Nestor PJ. In Vivo MRI Mapping of Brain Iron Deposition across the Adult Lifespan. J Neurosci. 2016;36:364-74.
[7] Mykola P, Svyrydova N, Trufanov Y. Susceptibility-weighted imaging and transcranial Doppler ultrasound in patients with cerebral small vessel disease. Neurological Sciences. 2020;41:2853-8.
[8] Pizarro-Galleguillos BM, Kunert L, Brüggemann N, Prasuhn J. Iron- and Neuromelanin-Weighted Neuroimaging to Study Mitochondrial Dysfunction in Patients with Parkinson's Disease. Int J Mol Sci. 2022;23.
[9] Wu T-T, Gao Y, Zheng Y-Y, Ma Y-T, Xie X. Atherogenic index of plasma (AIP): a novel predictive indicator for the coronary artery disease in postmenopausal women. Lipids in Health and Disease. 2018;17:197.
[10] Conklin J, Frosch MP, Mukerji S, Rapalino O, Maher MD, Schaefer PW, et al. Cerebral microvascular injury in severe COVID-19. medRxiv. 2020:2020.07. 21.20159376.
[11] Gregoire SM, Chaudhary UJ, Brown MM, Yousry TA, Kallis C, Jäger HR, et al. The Microbleed Anatomical Rating Scale (MARS): reliability of a tool to map brain microbleeds. Neurology. 2009;73:1759-66.
[12] Abou Elmaaty AA, Zarad CA. Role of magnetic susceptibility-weighted imaging in characterization of cerebral microbleeds in acute ischemic stroke Egyptian obese patients. The Egyptian Journal of Neurology, Psychiatry and Neurosurgery. 2020;56:72.
[13] Wiegertjes K, Ter Telgte A, Oliveira PB, van Leijsen EM, Bergkamp MI, van Uden IW, et al. The role of small diffusion-weighted imaging lesions in cerebral small vessel disease. J Neurol. 2019;93:1627-34.
[14] Rudilosso S, Chui E, Stringer MS, Thrippleton M, Chappell F, Blair GW, et al. Prevalence and significance of the vessel-cluster sign on susceptibility-weighted imaging in patients with severe small vessel disease. J Neurol. 2022;99:440-52.
[15] Pantoni L. Cerebral small vessel disease: from pathogenesis and clinical characteristics to therapeutic challenges. Lancet Neurol. 2010;9:689-701.
[16] Taoka T, Fukusumi A, Miyasaka T, Kawai H, Nakane T, Kichikawa K, et al. Structure of the medullary veins of the cerebral hemisphere and related disorders. Radiographics. 2017;37:281-97.
[17] Abou Elmaaty AA, Zarad CA. Role of magnetic susceptibility-weighted imaging in characterization of cerebral microbleeds in acute ischemic stroke Egyptian obese patients. Egypt J Neurol Psychiatr Neurosurg. 2020;56:1-9.
[18] Mitaki S, Takayoshi H, Nakagawa T, Nagai A, Oguro H, Yamaguchi S. Metabolic syndrome is associated with incidence of deep cerebral microbleeds. PLoS One. 2018;13:183-94.